

We are IntechOpen, the world's leading publisher of Open Access books Built by scientists, for scientists

4,800

Open access books available

122,000

International authors and editors

135M

Downloads

Our authors are among the

154

Countries delivered to

TOP 1%

most cited scientists

12.2%

Contributors from top 500 universities



WEB OF SCIENCE™

Selection of our books indexed in the Book Citation Index
in Web of Science™ Core Collection (BKCI)

Interested in publishing with us?
Contact book.department@intechopen.com

Numbers displayed above are based on latest data collected.
For more information visit www.intechopen.com



Superhard Superconductive Composite Materials Obtained by High-Pressure-High-Temperature Sintering

Sergei Buga, Gennadii Dubitsky, Nadezhda Serebryanaya,
Vladimir Kulbachinskii and Vladimir Blank
*Technological Institute for Superhard and Novel Carbon Materials,
Ministry of Education and Science of the Russian Federation
Russian Federation*

1. Introduction

Superhard superconducting materials are of considerable interest for the creation of high pressure devices for investigating electrical and superconducting properties of various materials. The superconducting composites consisting of superconductors and superhard materials that are in thermal and electrical contacts may satisfy very conflicting requirements imposed on superconducting materials for special research cryogenic technique, wear-resistive parts of superconductor devices, superconducting micro-electro-mechanical systems (MEMS), etc. The design of materials combining such properties as superconductivity, superhardness, and high strength is an interesting task for both scientific and applied reasons. Superconducting composites may be used for the production of large superconducting magnetic systems (Gurevich et al., 1987).

The discovery of superconductivity in heavily boron-doped diamonds (Ekimov et al., 2004; Sidorov et al., 2005) has attracted much attention. Superconducting diamonds are the hardest known superconductors. The potential applications of superconducting diamonds are broad, ranging from anvils in research high-pressure apparatus to superconducting MEMS. However, the highest value of the superconductivity onset temperature in boron-doped diamonds was found just about 7 K in thin CVD-grown films (Takano et al., 2004) and at about 4 K in bulk diamonds grown at high-pressure and high-temperature (Ekimov et al., 2004; Sidorov et al., 2005). In these pioneering works bulk polycrystalline diamonds with micron grainsize have been synthesized from graphite and B₄C composition (Ekimov et al., 2004) and graphite with 4 wt% amorphous boron (Sidorov et al., 2005). The synthesis have been carried out at 8-9 GPa pressure and 2500-2800 K temperature in both cases. Later Dubrovinskaya et al., 2006, carried out synthesis of graphite with B₄C composition at much higher pressure value 20 GPa but the same temperature of 2700K and found the superconducting state transition at lower temperature 2.4 - 1.4 K in the obtained doped polycrystalline diamonds. Due to the sharpening of the temperature interval of the superconductivity transition in magnetic field they suggested that superconductivity could arise from filaments of zero-resistant material. An alternative method for the creation of composite diamond superconductors was suggested by one of the authors of the present

article, G. Dubitsky, who used sintering of diamond powders with molybdenum to fabricate special research high-pressure anvils with $T_C = 10$ K (Narozhnyi et al., 1988). Such a unique high-strength superconducting anvils for research high-pressure apparatus were employed for investigations of the pressure effect up to 22 GPa on the superconductor transition temperatures in the metallic high-pressure phase of GaP. Modern technologies for large-scale industrial powder diamonds and cubic boron nitride manufacturing provide an easy opportunity to produce a wide range of superhard sintered superconductors with various mechanical and electronic properties.

By sintering diamond micropowders with metal powders (Nb, Mo) and using metal-coated diamond micropowders at high static pressure and temperature we obtained superhard superconductors with T_C substantially higher than in boron-doped diamonds (Dubitsky et al., 2005, 2006). Interacting with diamond, Nb and Mo metals form carbides bonding diamond crystallites into a united compact material having relatively high critical temperatures of the transition to the superconducting state.

The alternative route is the sintering of superconductor powders with superhard fullerites - new carbon materials produced from C_{60} and C_{70} fullerenes (Blank et al., 1998, 2006). Under high pressure and temperature treatment soft C_{60} and C_{70} powders transform into fullerene polymers and other carbon structures with various hardness including superhard and even superior to diamond. There are known many alkali metal-fullerene superconductors with relatively high T_C up to about 30K (Holczer & Whetten, 1993, Kulbachinskii, 2004, Kulbachinskii et al., 2008). However alkali metal-fullerenes react with oxygen when exposed to air. Sintering with inert superhard materials may protect such compounds from oxidation and provide superconducting properties of such superhard composites.

The highest critical temperature of superconductor transition among known "regular" superconductors has magnesium diboride MgB_2 with $T_C = 39$ K. The superconductor composites based on MgB_2 and superhard materials are promising materials as well (Kulbachinskii et al., 2010).

Using high-pressure-high-temperature sintering method we manufactured the following composite superhard superconducting materials: diamond-Nb, diamond-Mo, diamond- MgB_2 , cubic boron nitride- MgB_2 , fullerite C_{60} - MgB_2 , diamond- $Ti_{34}Nb_{66}$, diamond- Nb_3Sn , what will be described in this chapter.

2. Experimental section

Experimental samples of the target materials were obtained by treatment at high static pressures and temperatures. The experiments were carried out using modified "anvils with cavity"-type high-pressure apparatus (Blank et al., 2007). Pressure value was calibrated by electrical resistance jumps in reference metals Ba (5.5 GPa), Bi (2.5, 2.7, 7.7 GPa), Pb (13 GPa) and ZnSe (13.7 GPa) at known phase transitions. The temperature graduation of the chambers was performed using Pt/Pt-10%Rh and W/Re thermocouples. The initial components were placed into a tantalum-foil shell of 0.1 mm thickness. Samples were heated by ac current through a graphite heater with a tantalum shell as a part of the sample system. The materials have been obtained at pressures in the range of 7.7 - 12.5 GPa and temperatures of 1373 - 2173 K. The heating time was 60 - 90 s. The samples were quenched under high pressure with a rate of 200 K per second. After pressure release the samples were extracted from the high-pressure cell. Small cylinder-shaped samples with a diameter of 4.5 mm and a height of 3.5 mm were obtained. The parallelepiped samples $3.9 \times 2.51 \times 1.54$

mm³ size were made by laser cutting and polishing. The examples of optical images of polished surfaces for 2 different samples are presented in Fig. 1.

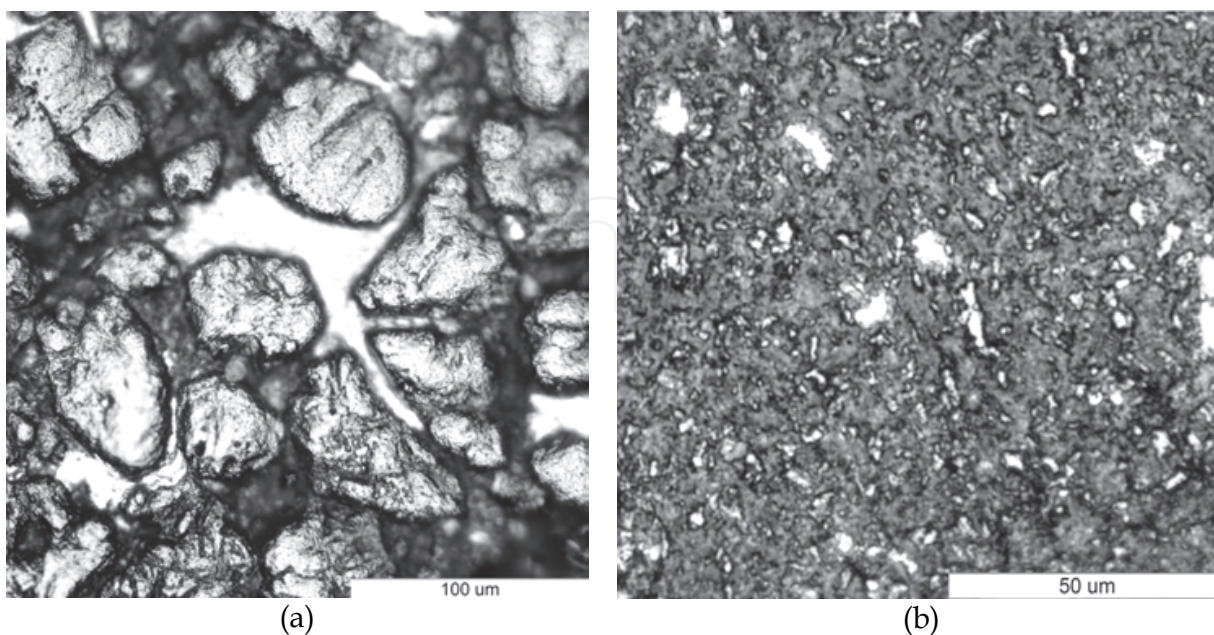


Fig. 1. The examples of images of the polished surfaces of diamond-Nb sample (a) and micro-nanodiamond-NbTi sample (b).

The pictures show grains of superhard compound like diamonds and superconducting compounds like metal alloys in between the grains. The X-ray diffraction analysis revealed formation of metal carbides on the boundaries of diamond micro- and nanocrystals and nanocarbon phases originated from C₆₀ fullerene in the samples synthesized with C₆₀ powder. The carbide phases provide strong chemical bonding of superconductor matrix with superhard carbon grains, thus the target composites possess very high strength.

We investigated the phase content of the samples by the powder X-ray diffraction method using an ARL X'TRA diffractometer with Si-Li semiconductor detector and Cu K α radiation ($\lambda = 0.1541$ nm) source. The electrical resistance of the resulting samples was measured by the conventional four probe method. Electrical contacts were made using conducting silver paste. The temperature dependence of the resistance was measured in the interval $1.7 < T < 300$ K. We applied the magnetic field up to 5T to determine the effect of magnetic field on the superconductivity transition temperature.

The Vickers microhardness was measured using PMT-3 device at an indenter load of 5.5 N. Sound velocities in 3 samples were measured using a wide-field pulse scanning acoustical microscope (WFPAM) in reflection mode (time-of-flight method) at a driving frequency of 50 MHz. The mean diameter of the acoustic beam in the specimen was about 0.1 mm. This experimental procedure was described in detail in (Prokhorov et al., 1999).

3. Superhard material-superconductive metal-systems

3.1 Diamond-niobium system

Synthetic diamond powder with 80 – 100 μm crystallites covered with a niobium film by vacuum sputtering was used as the initial material. The total amount of niobium in the initial material was 24 wt %. The experiments were carried out at a pressure of 7.7 GPa and a temperature of 1973 K for 60 s. The diffraction patterns exhibited peaks associated with

diamond and NbC monocarbide (Fig. 2). A small fraction of NbO₂, practically traces, was also found. The NbC monocarbide synthesized at the boundaries of the crystallites had a face-centered cubic lattice with the cubic parameter $a_0 = 0.447$ nm. This value is consistent with the data obtained for NbC by another method (Toth, 1971).

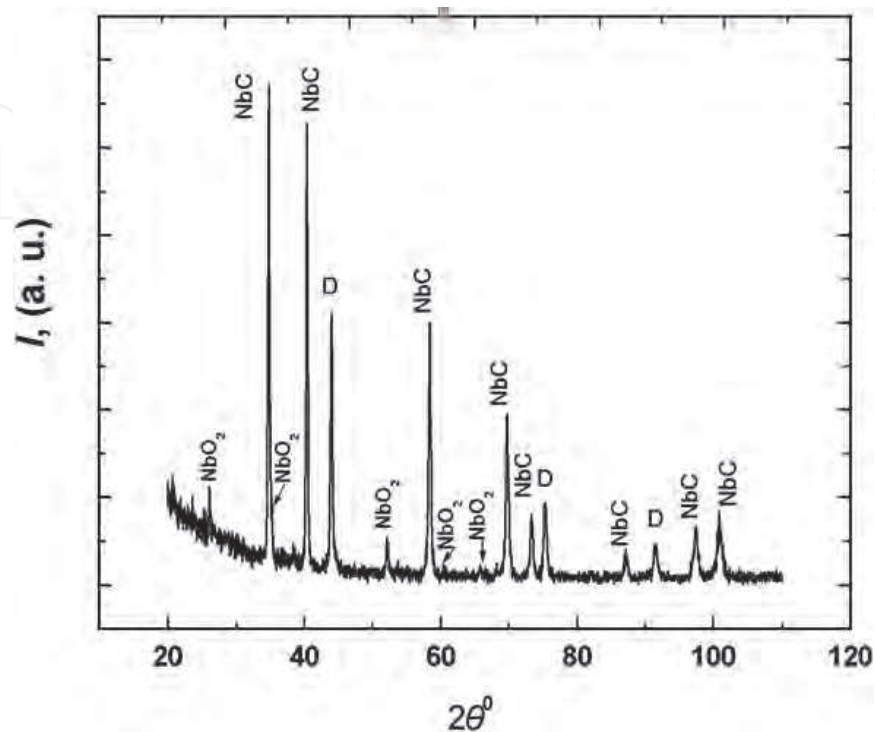
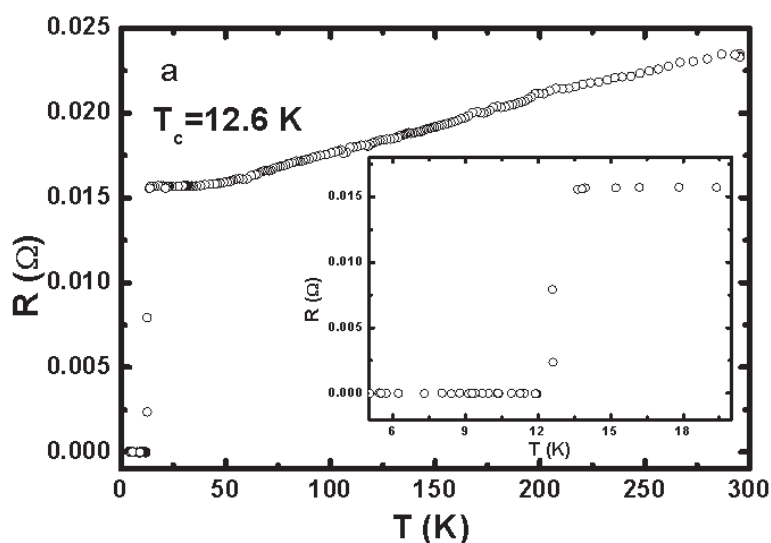


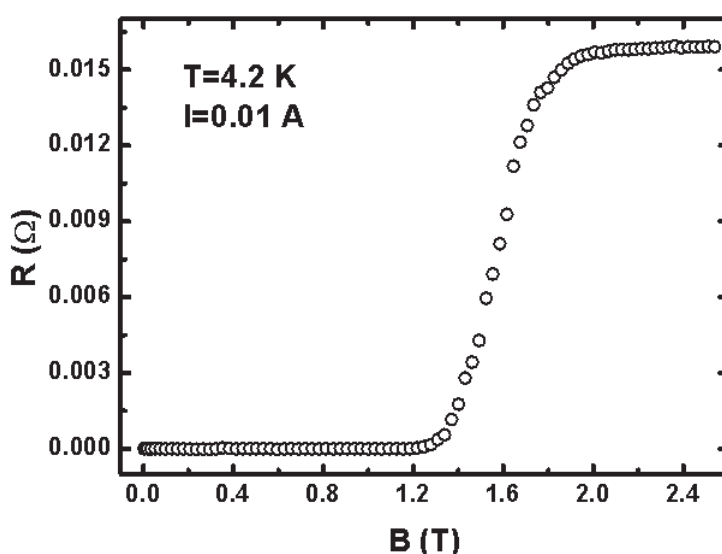
Fig. 2. X-ray diffraction pattern of sintered diamond-niobium sample. Diffraction reflections of NbC, diamond and NbO₂ are denoted.

The critical temperature of the transition to the superconducting state in all the measurements was fixed at the onset of the transition. According to an analysis of the temperature dependence of the resistance, the critical temperature of the transition of the synthesized samples to the superconducting state was equal to $T_C \approx 12.6$ K (Fig. 3a), which is characteristic of a NbC compound with almost full carbon positions (Karimov & Utkina, 1990; Shabanova et al., 1996; Krasnosvobodtsev et al., 1995). Carbon deficient NbC_{1-x} having lower T_C or superconductivity was entirely absent. The characteristic feature of the synthesized samples is a quite narrow superconducting transition, $\Delta T \approx 1.5$ K. The measured dependence of the resistance of a sample on the external magnetic field (Fig. 3b) is characteristic of NbC carbide. The value of the second critical field $H_{C2} = 1.25$ T (at $T = 4.2$ K) is consistent with H_{C2} for NbC films obtained by the laser-evaporation method (Shabanova et al., 1996). Thus, one may conclude that crystallites NbC with an almost perfect crystal structure were formed on the surface of the sintered diamond and a low concentration of defects has place in NbC which reduces the temperature of the superconducting transition (Pickett et al., 1986). An insignificant admixture of NbO₂ had no effect on the critical temperature of samples.

The microhardness values varied in the range of 35 -95 GPa depending on the actual place of indentation (Dubitski et al., 2005, 2006). According to (Toth, 1971), the Vickers microhardness of NbC is approximately equal to 17 GPa. This value is significantly lower than the results obtained in our work for microdomains enriched in NbC. The hardness of



(a)



(b)

Fig. 3. Temperature (a) and magnetic field (b) dependences of the resistance for the sample obtained in the diamond-niobium system.

	ρ g cm ⁻³	V_L km s ⁻¹	V_T km s ⁻¹	E GPa	B GPa	G GPa	σ
Diamond-Nb	4.1± 0.1	12.1± 0.5	6.9± 0.25	490± 95	340± 30	195± 14	0.26± 0.04
Polycrystalline diamond "carbonado"	3.74± 0.05	16± 0.5	9.6± 0.3	850± 120	490± 30	340± 24	0.22± 0.04

Table 1. Diamond-Nb density ρ , longitudinal and transverse sound velocities V_L , V_T , Young modulus E , bulk and shear elastic modules B , G and the Poisson ratio σ . Data for polycrystalline sintered diamond "carbonado" type are given for reference.

such microdomains is high apparently due to the effect of the of diamond crystallites, which have much higher hardness (100 - 150 GPa along different faces, depending on the quality of the crystals). The velocities of sound and the elastic modules are 30 - 40% less than in pure bulk polycrystalline diamond (Table 1). Nevertheless they are comparable with the values for the next very strong superhard material: cubic boron nitride (c-BN).

3.2 C₆₀-diamond-niobium system

High-pressure - high-temperature treatment of C₆₀ and C₇₀ fullerenes leads to polymerization and transformation into new metastable carbon structures (Blank et al., 1998, 2006). Among various polymeric forms, the 3D-polymeric ones are the hardest

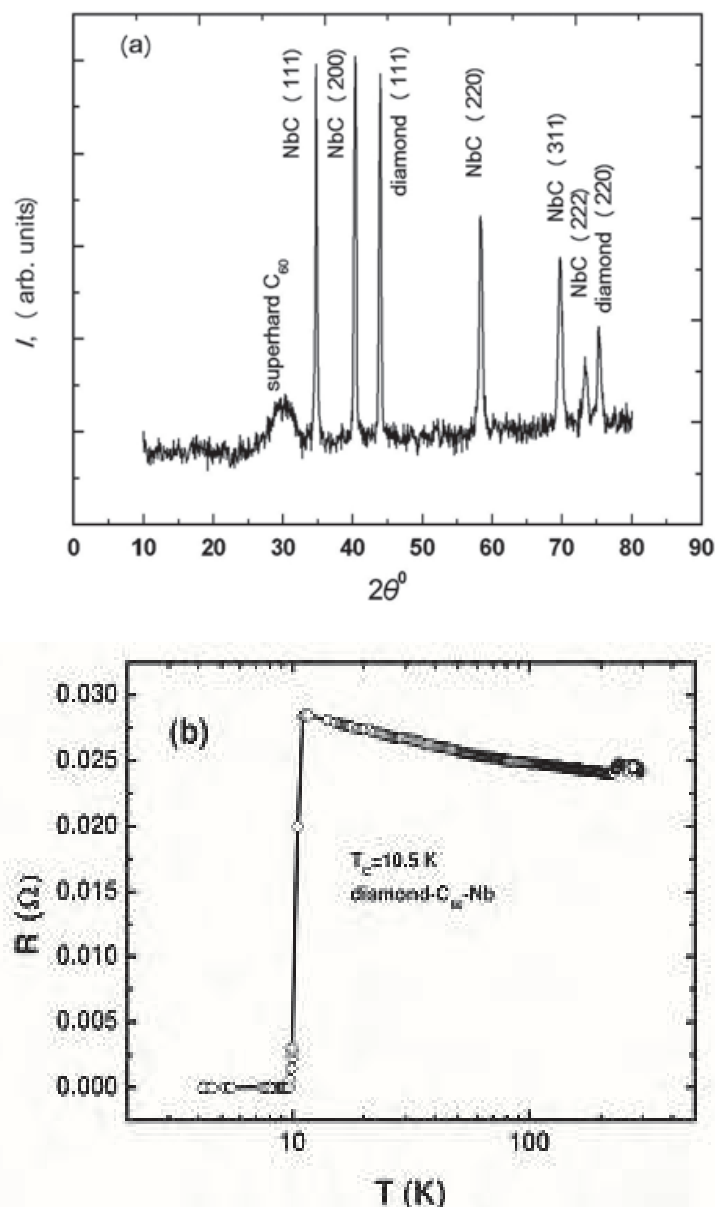


Fig. 4. The X-ray diffraction pattern (a) and the temperature dependence of the resistance (b) for the sample obtained in the C₆₀- diamond-niobium system.

(Blank et al., 1998). The density of superhard ($H_v > 50$ GPa) and ultrahard ($H_v > 120$ GPa) forms ranges from 2.5 to 3.3 g cm⁻³, intermediate between the densities of graphite and diamond. Mechanical, electrical and other properties of such materials strongly depend on their particular crystalline or disordered structure. A set of metal-C₆₀ compounds are superconducting with $T_C = 2 - 34$ K (Holczer & Whetten, 1993). However the conventional fullerene superconductors are not hard and chemically reactive; they oxidize in air. We investigated the synthesis of composite superconductors on the basis of a 50%-50% mixture of C₆₀ powder with niobium coated diamond powder (Dubitsky et al., 2006) as described in the part above. Sintering was carried out at a pressure of 12.5 GPa and temperature 1650 K. The XRD analysis (Fig. 4a) showed formation of a disordered superhard component on the basis of C₆₀ (broad diffraction peak) and niobium monocarbide with diamond crystals. The microhardness values of this composite material was 45 - 95 GPa. It is superconducting below 10.5 K (Fig. 4b).

3.3 Diamond-molybdenum system

In this system, a synthetic-diamond powder with a granularity of 40 - 100 μm and a molybdenum powder with a particle size of 1 - 5 μm were used as the initial materials consisting of 60 wt % of diamond and 40 wt % of molybdenum. A compact material was obtained by holding at a pressure of 7.7 GPa and a temperature of 2173 K for 90 s. The phase content of the samples was determined by the same method as for the diamond-Nb system. The following phases were identified in the samples: the diamond, the α -MoC phase with a cubic lattice with the parameter $a_0 = 0.427$ nm (B1 type), the η -MoC hexagonal phase with the lattice parameters $a_0 = 0.300$ and $c_0 = 1.452$ nm, and traces of the hexagonal γ -MoC phase (WC type) with the parameters $a_0 = 0.290$ and $c_0 = 0.282$ nm. The lattice parameters that were determined for molybdenum-carbon compounds are consistent with the data published by (Toth, 1971). The Vickers microhardness of the samples varies in the range of 27 - 83 GPa.

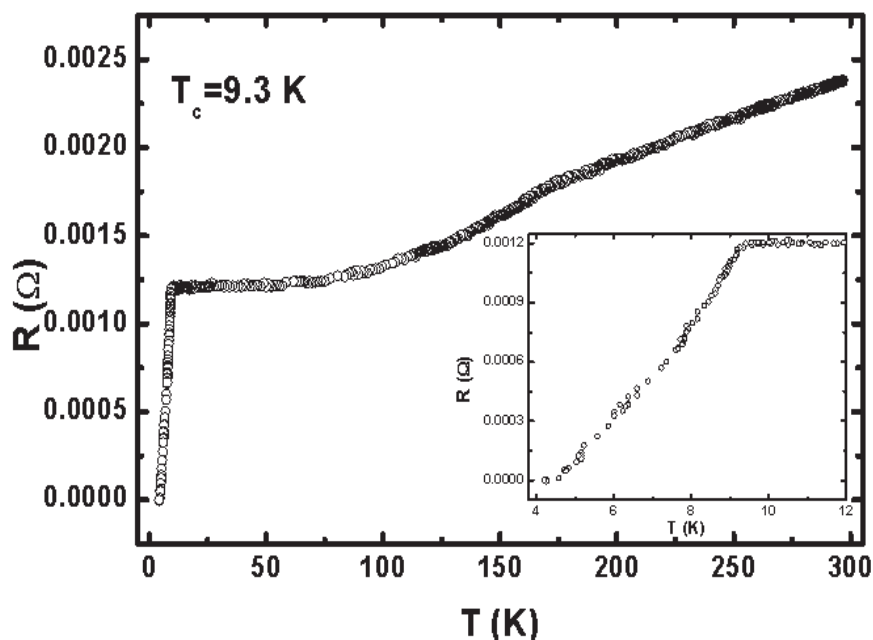


Fig. 5. Temperature dependence of the resistance for the sample obtained in the diamond-molybdenum system.

The composites obtained in the reaction of diamonds with molybdenum are superconductors with characteristic features. First, the onset of the transition to the superconducting state is $T_C = 9.3$ K, which is slightly lower than the T_C values for molybdenum carbide obtained by sintering powders of molybdenum and graphite (Willens et al., 1967). Second, the transition width $\Delta T \approx 5$ K is larger than that for the diamond-niobium system. Fig. 5 shows the temperature dependence of the resistance of these composites.

4. Superhard material-MgB₂-systems

4.1 Diamond-MgB₂ and cubic boron nitride-MgB₂-systems

Magnesium diboride, whose superconductivity was discovered 10 years ago (Nagamatsu et al., 2001; Zenitani & Akimitsu, 2003) has much higher critical temperature $T_C = 39$ K than niobium carbide and molybdenum carbide. Many investigations were devoted to the effect of the conditions of MgB₂ producing and treatment at high pressures and temperatures on the superconducting properties with various dopants (Jung et al., 2001; Prikhna et al., 2002; Pachla et al., 2003; Tampieri et al., 2004; Toulemonde et al., 2003; Zhao et al., 2003; Dou et al., 2003). It is of interest to obtain a superconducting composite material in which diamond or cubic boron nitride are used as the superhard components and MgB₂ is used as the superconducting component.

As the initial material, we used industrial MgB₂ powders in which the content of the basic product was equal to 98.5%. The particle size was reduced to 5 – 10 μm by additional powdering. The prepared mixtures consisted of 80 wt % of the superhard component and 20 wt % of MgB₂. The granularity of the diamond and cubic boron nitride powders was equal to 40 – 100 and 28 – 40 μm , respectively. The assembly of the high-pressure cells and the experimental procedure were the same as those used for the diamond-molybdenum system. In one of the experiments, a niobium-coated diamond powder was used. The samples were obtained by sintering at a pressure of 7.7 GPa and a temperature of 1373 K for 60 s.

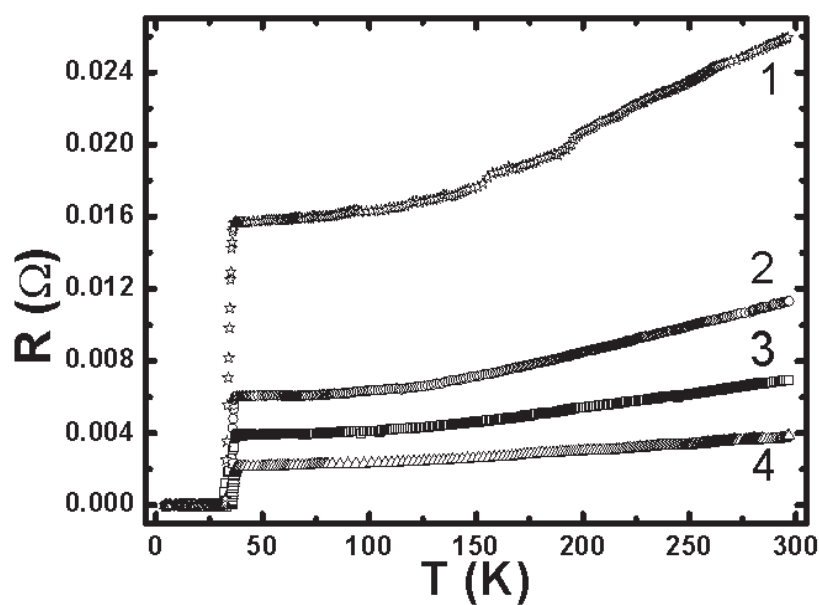
Using XRD analysis, diamond, MgB₂ and MgO were identified in the system diamond-MgB₂ after the synthesis.

The temperature dependence of the resistance of the samples shows that the temperature of the transition to the superconducting state is $T_C \approx 37$ K (Fig. 6), which is close to the value known for MgB₂ (Nagamatsu et al., 2001). This closeness indicates that MgB₂ has a key role in the superconductivity of these composite materials, and the matrix consisting of cubic boron nitride or diamond changes T_C insignificantly, while the hardness of such superconducting material is much higher than the one of compacted MgB₂.

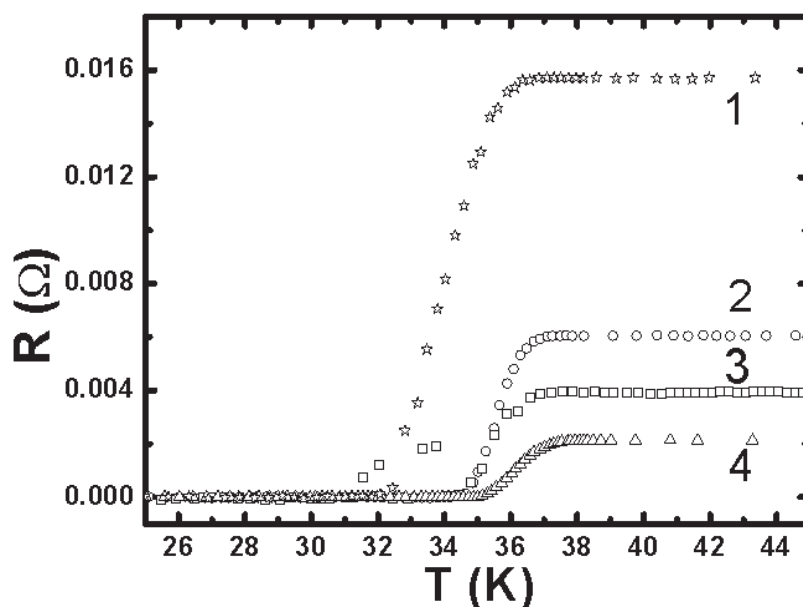
The microhardness of the samples indicates that the composite matrix (consisting of cubic boron nitride or diamond) occupying the major part of the body of the samples has a

	ρ , g cm ⁻³	V_L , km/s	V_T , km/s	E , GPa	B , GPa	G , GPa	σ	H_v
Diamond- MgB ₂	3.4±0.1	5.6±0.3	3,3±0.15	90±20	57±4	35±3	0.23±0.04	25÷78
cBN - MgB ₂	3.3±0.1	6.0±0.3	3.7±0.15	110±25	60±7	45±4	0.19±0.04	24÷57

Table 2. Diamond- MgB₂ and cBN-MgB₂ composites density ρ , longitudinal and transverse sound velocities V_L , V_T , Young modulus E , bulk and shear elastic modules B , G and Poisson ratio σ and the Vickers microhardnes H_v .



(a)



(b)

Fig. 6. Temperature dependence of the resistance (a) and transition range (b) for the composite samples obtained in the systems (1) cubic boron nitride-MgB₂, $T_C = 36.1$ K, (2) diamond-MgB₂, $T_C = 36.9$ K, (3) MgB₂, $T_C = 37$ K, and (4) diamond-niobium-MgB₂, $T_C = 37.5$ K.

microhardness of 57 – 95 GPa. Such microhardness values are characteristic for superhard compact polycrystalline materials based on cubic boron nitride and diamond that are used to produce various abrasive and cutting tools (Shul'zhenko et al., 1987). The specific gravity and velocities of longitudinal and transverse sound waves were measured and elastic modules evaluated (Table 2). Though the elastic modules are not very high, such materials have good potential for applications.

4.2 Polymerized fullerite C₆₀-MgB₂- system

We synthesized and investigated a set of composite materials obtained from MgB₂ superconductor and C₆₀ fullerite mixed in various bulk ratios (Kulbachinskii et al., 2010). The same commercial MgB₂ powder with 98.5% of MgB₂ and commercial C₆₀ powder with 99.8% C₆₀ and the rest 0.2% of other carbon components were used as the initial compounds for the synthesis. The superconducting superhard composite possesses superconductivity due to MgB₂ fraction and superhardness due to polymerized C₆₀ part (Blank et al., 1998).

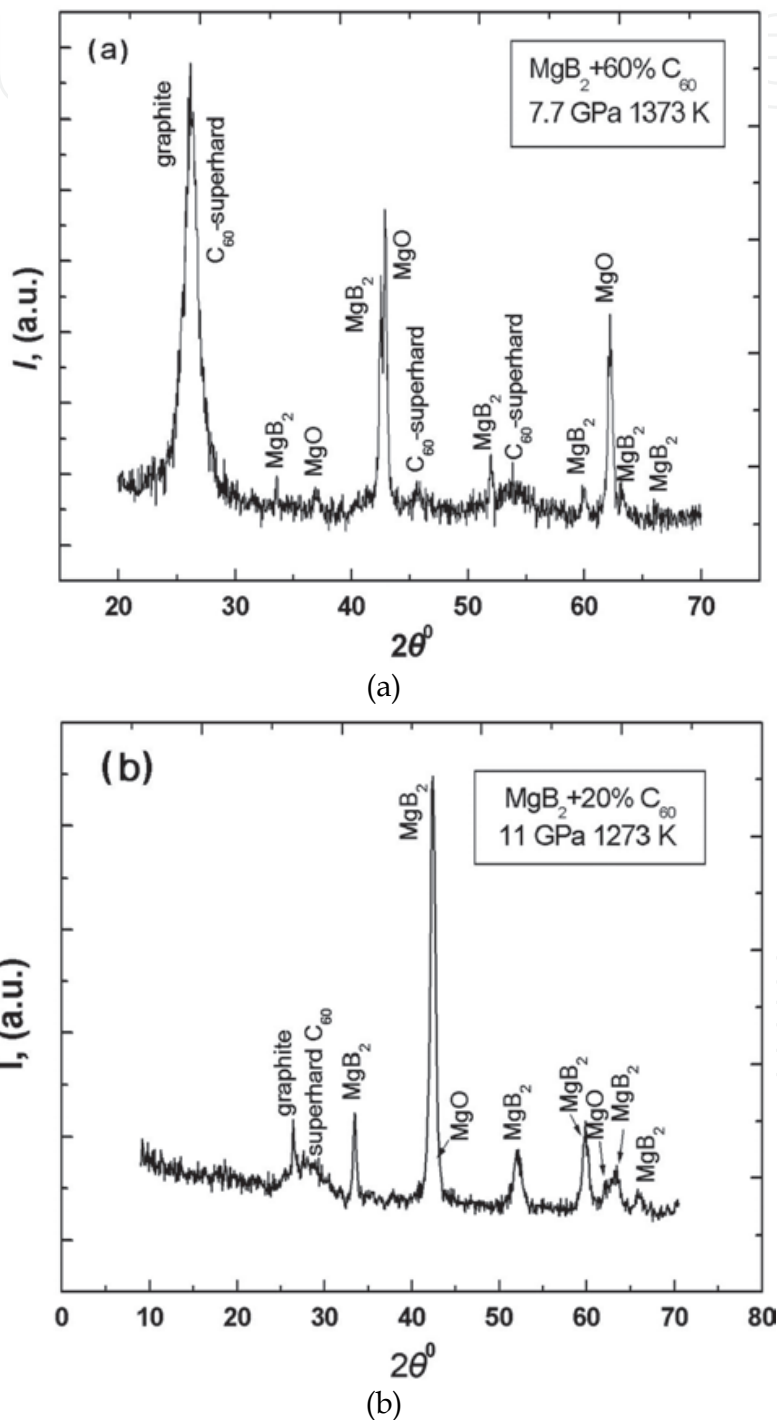
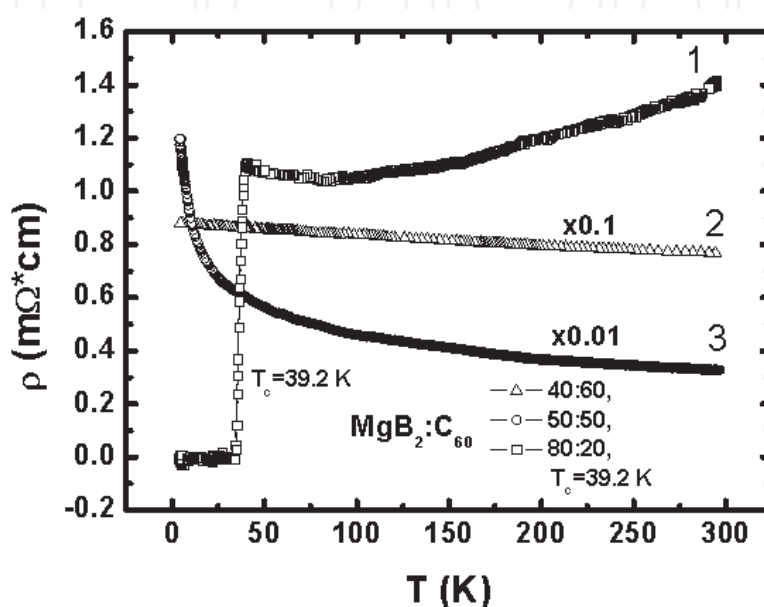
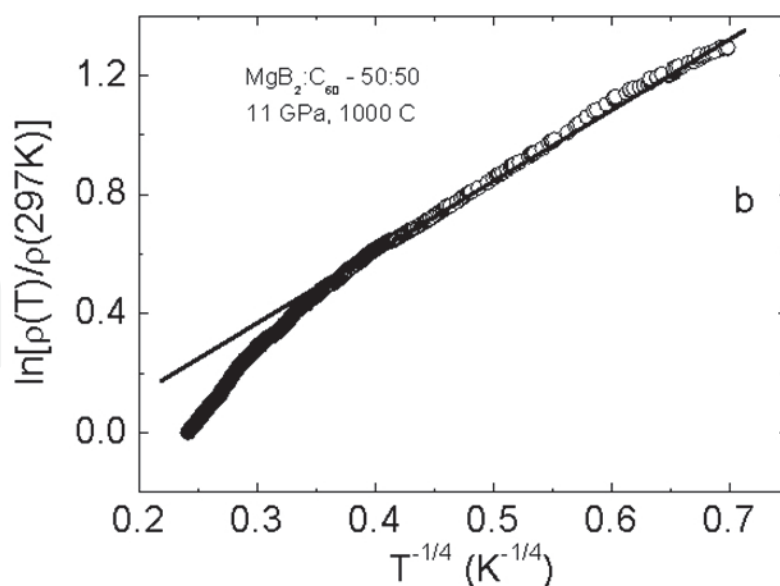


Fig. 7. Diffraction data composites MgB₂:C₆₀. Parameters of synthesis are shown at figures.

The particle size was reduced to 5–10 μm by additional powdering. We prepared polycrystalline composite $\text{MgB}_2\text{:C}_{60}$ with different wt. content of C_{60} up to 60%. The samples of the materials were obtained at high static pressures 7.7 GPa and temperatures 1273 - 1373 K. The Vickers microhardness values of composites $\text{MgB}_2\text{-C}_{60}$ were in the range of 18 - 59 GPa. The lowest value has been measured at the local point with dominating MgB_2 grains and the highest ones at the point with dominating superhard compound. According to (Prikhna et al., 2002), the Vickers microhardness H_V of MgB_2 with 2 wt. % of Ta synthesized at $T_s=1073$ K and $P = 2$ GPa was approximately equal to 12.8 GPa. In samples of composites



(a)



(b)

Fig. 8. a) Temperature dependence of resistivity for composites with different content $\text{MgB}_2\text{:C}_{60}$: 1 - 80:20; 2 - 40:60; 3 - 50:50 wt%; b) logarithm of the relative change of the resistivity versus $T^{-1/4}$.

MgB₂:C₆₀ we identified MgB₂, MgO and superhard 3D-polymerized C₆₀. MgO was revealed in the initial magnesium diboride, its content increased with the increasing of sintering temperature. In Fig. 7 diffraction data are shown for two samples with different MgB₂:C₆₀ ratio.

It was found that up to 20 wt. % C₆₀ the composite MgB₂:C₆₀ is a superconductor. The superconducting transition temperature of composite MgB₂:C₆₀ - 80%:20% is $T_c=39,2$ K, that is the same as for host MgB₂ ($T_c \approx 39$ K (Nagamatsu et al., 2001)). In Fig. 8 we plotted temperature dependences of resistivity for composites with different C₆₀ content.

The resistivity of the superconducting composite MgB₂:C₆₀-80%:20% increases near the transition to the superconducting state ($39 < T < 80$ K). It is not typical for the host MgB₂. We suppose that in this temperature range C₆₀ clusters play a significant role in the temperature dependence of the resistivity. For clusters of C₆₀ the resistivity increases when temperature decreases (Buga et al., 2000, 2005).

When the content of C₆₀ increases above 20 wt. %, the superconductivity disappears and the temperature dependence of the resistivity changes. Mott variable range hopping conductivity was observed, following the law:

$$\sigma = \sigma_0 \exp\left\{-\left(T_0 / T\right)^{1/4}\right\}$$

Fig. 8b. shows the relative change of resistivity in logarithmic scale on $T^{-1/4}$. The linear dependence is clearly visible in the temperature range 4.2- 60 K. When the content of C₆₀ is >60 wt. % the resistivity slowly increases with the temperature decrease as it is shown in Fig. 8 for sample MgB₂:C₆₀-40%:60%. This takes place because the main superhard carbon component which appeared after C₆₀ transformation has graphite-like cross-linked layered structure with semimetallic type of conductivity (Buga et al., 2000) .

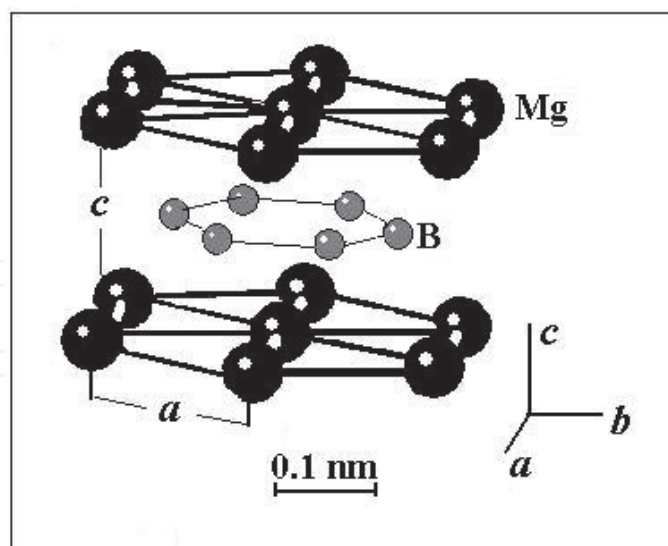


Fig. 9. The crystal structure of MgB₂. Axes of hexagonal unit cell a and c are designated.

MgB₂ has hexagonal crystal structure ((Nagamatsu et al., 2001). This structure (Fig. 9) consists from a sequence of hexagonal closed packed layers of Mg and graphite-like layers of B. In such structure atoms of Mg have ionic bonding with atoms of B. Inside the boron layer B atoms have covalent 2D bonding.

The critical field value B_c^c for magnetic field parallel to c axis is about 3–4 T down to $T = 0$ K (Lyard et al., 2002). The value of in plane critical magnetic field B_c^{ab} in the ab plane is significantly higher and reaches 15–20 T at $T=0$ K. The anisotropy coefficient is equal $B_c^{ab}/B_c^c = 4-5$. In the superconducting composite $MgB_2:C_{60}$ -80%:20% we measured superconducting transition at different magnetic fields. (Fig. 10a). Using these data the temperature dependence of the critical magnetic field B_c was plotted in Fig. 10b. The temperature dependence of B_c is close to the same dependence in the initial MgB_2 (Lyard et al., 2002; Buzea & Yamashita, 2001). Thus composite with 20 wt. % of C_{60} has the same superconducting parameters as host MgB_2 .

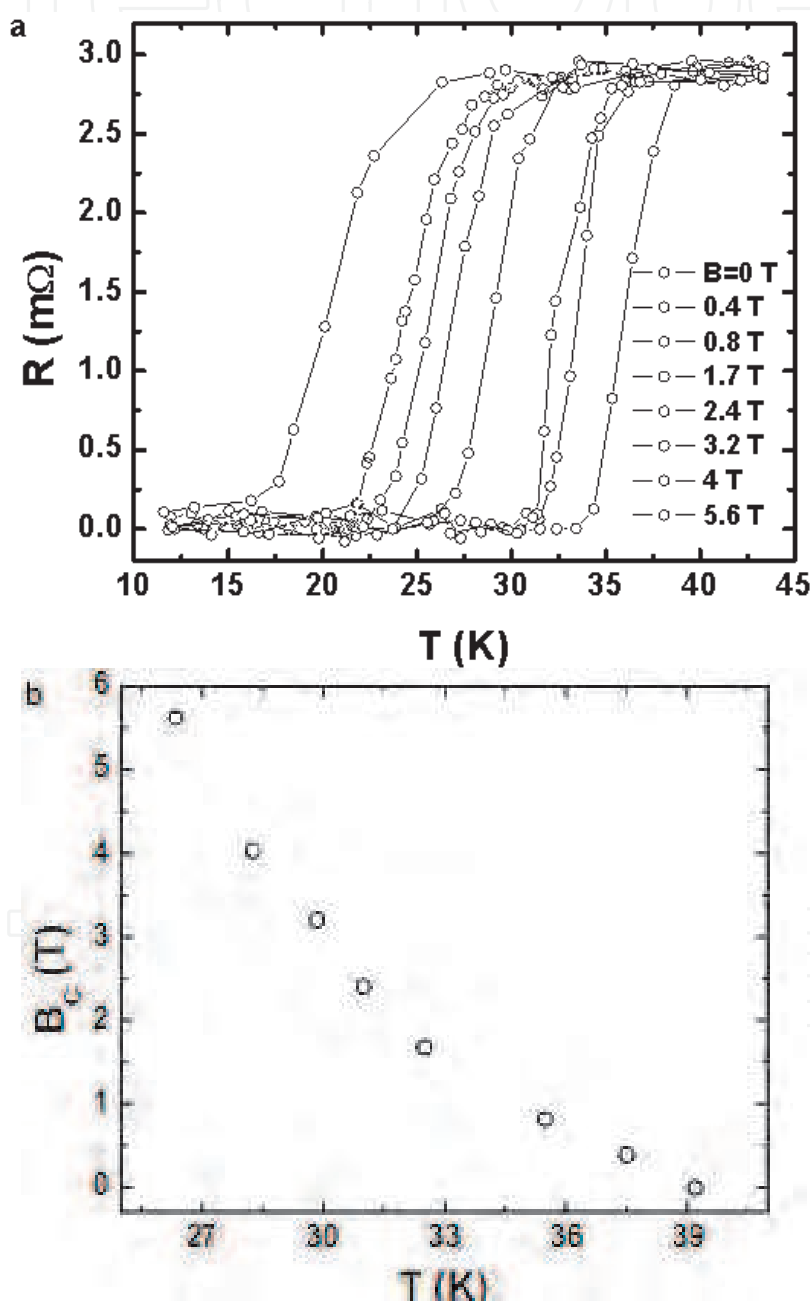
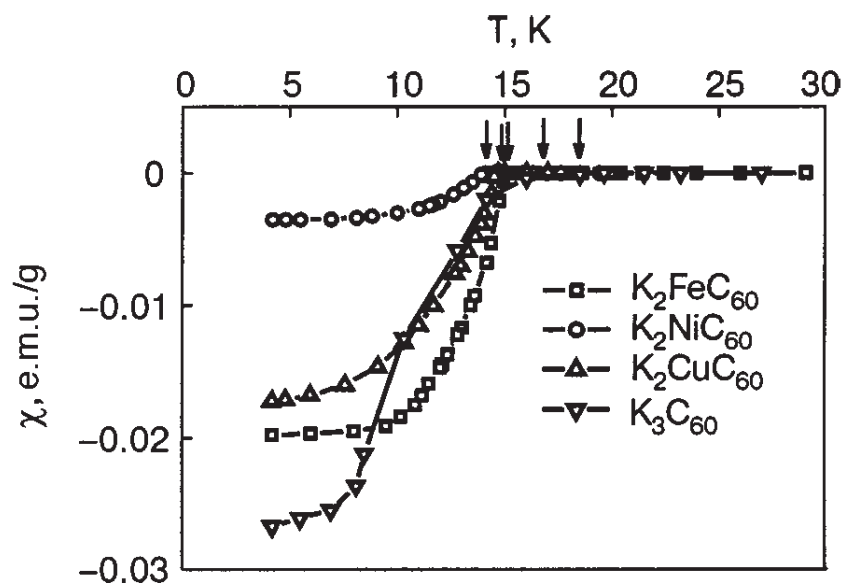


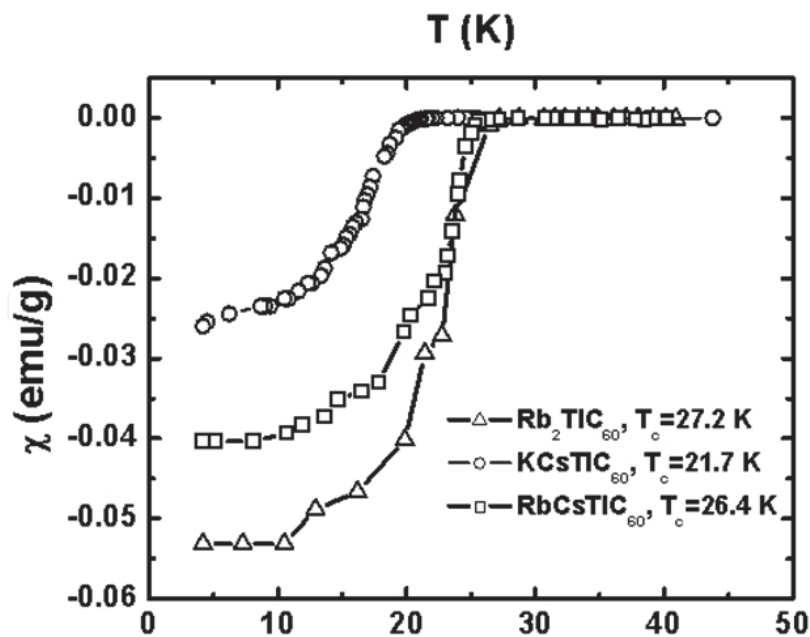
Fig. 10. Temperature dependence resistance of R for $MgB_2:C_{60}$ - 80:20 wt. % at different magnetic field (a), and temperature dependence of critical magnetic field B_c (b) that is similar to that of the initial MgB_2 .

4.3 Superconductivity of heterofullerides

Recently a method has been developed for synthesizing superconducting heterofullerides of the Fe and Cu groups with the composition K_2MC_{60} (Bulychev et al., 2004). For example, Fig. 11a shows the temperature dependence of the magnetic susceptibility χ for fullerides with $M=Fe, Ni, Cu$. Also shown in Fig. 11a is the $\chi(T)$ curve for the well-known superconductor K_3C_{60} for comparison. Superconducting heterofullerides of composition K_2MC_{60} have lower superconducting transition temperatures T_c than K_3C_{60} , and the crystal lattice constant a of



(a)



(b)

Fig. 11. Temperature dependence of the magnetic susceptibility χ of fullerides of composition K_2MC_{60} ($M = Fe, Ni, Cu$) and K_3C_{60} for comparison (upper) and compounds $RbCsTlC_{60}$, $KCsTlC_{60}$, Rb_2TlC_{60} (down).

the heterofullerides studied is smaller than that of K_3C_{60} , apparently because substitution of the potassium ion by an ion of smaller diameter decreases the lattice constant. Thus there is a correlation between the superconducting transition temperature and the crystal lattice constant: a decrease of a leads to a decrease of T_c .

Fullerides $RbCsTiC_{60}$ and Rb_2TiC_{60} have superconducting transition temperature $T_c = 26.4$ K, and 27.2 K respectively. For $KCsTiC_{60}$, the value of $T_c = 21.7$ K is the highest for fullerides with potassium atoms. Temperature dependences of the magnetic susceptibility of these compounds are plotted in Figure 11b. The fulleride $KCsTiC_{60}$ possesses the highest $T_c = 21.7$ K among all synthesized in the present study of heterofullerides with potassium. This confirms the suggestion that the increase of the T_c value is due to the increase of the lattice constant caused by substitution of K and Rb by Cs. $KCsTiC_{60}$ has maximal value of a ($a = 1.442$ nm compared to K_3C_{60} $a = 1.431$ nm) among all superconducting heterofullerides with potassium. The same is for $RbCsTiC_{60}$ ($a = 1.467$ nm, Rb_2BeC_{60} $a = 1.445$ nm). Such appreciable increase of the parameter a of face-centred cubic lattice is quite naturally and also is one more proof of intercalation of atoms of bigger sizes in fulleride structure. There were no superconducting transitions in heterofullerides with more than one Cs atom per fullerene C_{60} . It is of substantial interest to investigate sintering of such compounds with superhard materials like diamond and cBN to learn if superhard compounds protect superconducting metal-fullerene compound against oxydation and provide high mechanical properties of the composite.

5. $Ti_{34}Nb_{66}$ - and Nb_3Sn -diamond micropowder-systems

5.1 $Ti_{34}Nb_{66}$ -diamond system

The NbTi alloy is a superconductor which has one of the best strength and high critical magnetic field. A set of new composite materials were synthesized from $Ti_{34}Nb_{66}$ and Nb_3Sn superconductors mixed with microcrystalline diamond and nanodiamond powders in various bulk ratios. The particle size of superconductors was reduced to 5–10 μm by powdering.

The initial $Ti_{34}Nb_{66}$ alloy (Fig. 12) has a body-centered cubic crystal structure with $I m \bar{3} m$ space group and the unit cell parameter $a = 0.328$ nm. The superconducting temperature $T_c = 9.85$ K is known for this alloy.

The crystal structure of $Nb_{34}Ti_{66}$ is a homogeneous solid solution with statistical distribution of elements in a unit cell. Figure 13 shows diffractograms of samples obtained after sintering of the mixture of diamond powder and superconductor under pressure of 7.7 GPa at temperatures 1373 K and 1623 K. The lower diffractogram No. 4 (Fig. 13a) was obtained from the initial alloy, the next one (No. 3) of the sample obtained after sintering at 1373 K. No reflections of TiC or NbC appeared at this synthesis temperature.

The next two samples were sintered at 1623 K. The diffractogram No. 2 corresponds to the sample $Nb_{34}Ti_{66}$ (50%) mixed with 45% diamond micropowder covered by Nb and 5% of nanodiamond is added in this composition. The diffractogram No. 1 corresponds to the sample $Nb_{34}Ti_{66}$ (50%) mixed with 50% diamond micropowder. We will discuss in detail the difference of diffraction patterns of these samples and how it may affect on the superconductive transition temperature.

At the diffractograms of samples No. 1 and 2 the diffraction peaks from $Nb_{34}Ti_{66}$ alloy are easy visible because they have maximal amplitude. They are slightly shifted one to another and the shift is larger at wide angles ($2\theta \sim 90 \div 100^\circ$). A cubic unit cell parameter of $Ti_{34}Nb_{66}$

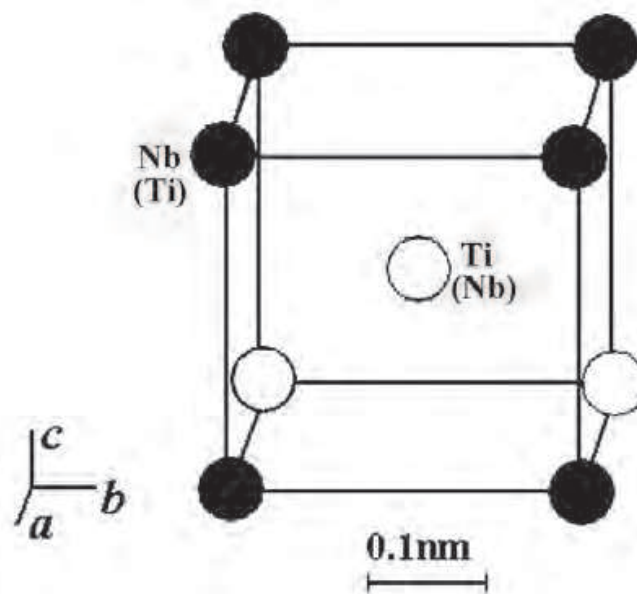


Fig. 12. The crystal structure of Nb₃₄Ti₆₆ alloy. Nb and Ti atoms have no determined positions.

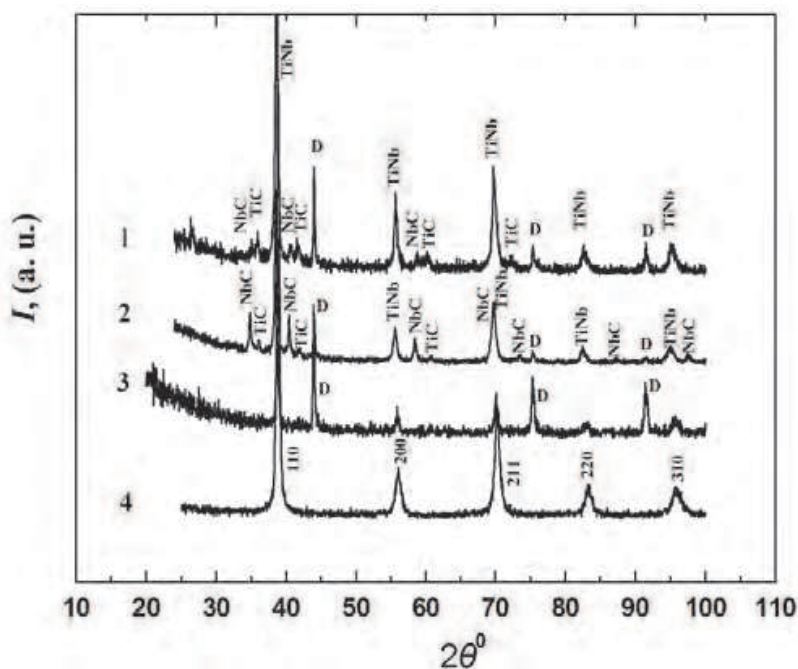
alloy calculated with the wide angles (see fig. 13) $a=0.329$ nm of sample No. 1 is slightly less than $a = 0.330$ nm of sample No. 2. The intensities of the main peaks are different in these two samples. The intensities of TiC and NbC peaks are different in these samples as well. In sample No. 1 the intensity of TiC-reflections is higher than NbC-reflections while in sample No 2 the intensity of NbC-reflections is higher than TiC-reflections. As for example, at $2\theta = 70\div 75^\circ$ and $85\div 90^\circ$ regions (Fig. 13b) NbC-reflections of diffractogram No. 1 disappear. The additional Nb covering diamond crystals in sample No. 2 leads to higher quantity of NbC in this sample. Apparently, 5% of nanodiamond in sample No. 2 increases a separation of Nb. Taking into account that the atomic radius of Ti (0.146 nm) is higher than the atomic radius of Nb (0.145 nm) and that the intensities of NbC - reflections increased, we suppose that the concentration of Nb in sample No. 1 is higher than in sample No. 2. That is why the cubic parameter is smaller. This leads to higher T_C in sample No 1 than in sample No. 2 (Fig. 14).

The appearance of NbC and TiC evidences partial decomposition of Nb₃₄Ti₆₆ alloy during the synthesis. Carbides were synthesized under high pressure 7.7 GPa without melting of metals though temperature of synthesis 1625 K is less than the necessary for direct synthesis of carbides. Their melting temperatures exceed 2000 K. The large part of carbon (50%) in samples promotes formation of carbides. However, the content of carbides is not sufficient to rise the T_C value up to 12.6 K known for NbC carbide.

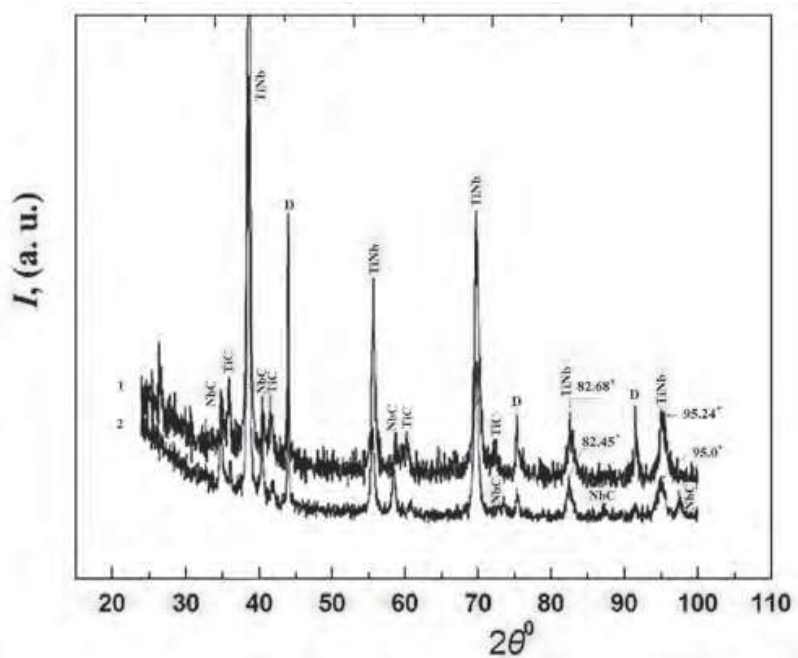
Table 3 shows the Vickers microhardness of Ti₃₄Nb₆₆ -diamond composite samples No's 1 and 2. The value of microhardness has a wide range as well as in the other composites: the lowest value of hardness has been measured for the Ti-Nb-alloy located in superconductive channels (35 GPa in sample No. 1 and 42 GPa in sample No. 2) and the highest ones in superhard matrix (93-98 GPa). We suppose that the higher hardness of channels (42 GPa) in sample No. 2 has place due to nanodiamond fraction in this sample.

No. 1: 50% Ti₃₄Nb₆₆ + 50% diamond micropowder, $T_C=8.9$ K;

No. 2: 50% Ti₃₄Nb₆₆ + 45% diamond micropowder covered by metallic Nb + 5% nanodiamond, $T_C=6$ K.



(a)



(b)

Fig. 13. (a) Diffractograms of ($\text{Ti}_{34}\text{Nb}_{66}$ + diamond micropowder) samples sintered at high pressure 7.7 GPa and high temperature 1373 K and 1623 K. The composition of samples: 1) 50% $\text{Ti}_{34}\text{Nb}_{66}$ + 50% diamond micropowder, $T=1623$ K; 2) 50% $\text{Ti}_{34}\text{Nb}_{66}$ + 45% diamond micropowder covered by Nb + 5% nanodiamonds, $T=1623$ K; 3) 50% $\text{Ti}_{34}\text{Nb}_{66}$ + 50% diamond micropowder, $T = 1373$ K; 4) initial $\text{Ti}_{34}\text{Nb}_{66}$ alloy.

(b) X-ray diffractograms of samples No's. 1 and 2. D - diffractonal reflections of diamond, NbC and TiC - diffractonal reflections from Nb and Ti carbides. TiNb and the wide angles of $2\theta^{\circ}$ are denoted for $\text{Ti}_{34}\text{Nb}_{66}$ reflections.

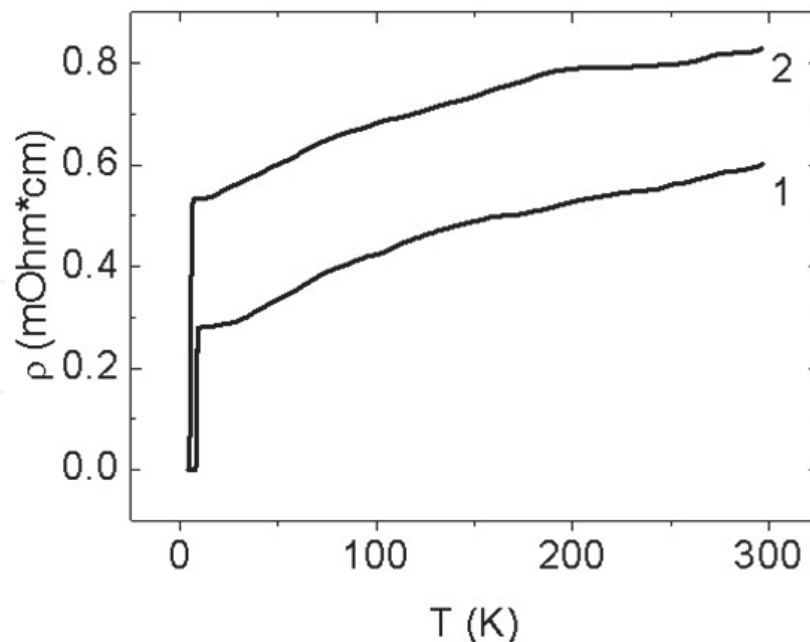


Fig. 14. Temperature dependence of resistance in two superhard composites sintered at $T = 1623$ K and $P = 7.7$ GPa.

Sample No.	Composite	Component ratio, wt. %	Vickers microhardness, GPa	T_c , K
1	$Ti_{34}Nb_{66}$ -diamond micropowder	50:50	35-93	8.9
2	$Ti_{34}Nb_{66}$ -(diamond micropowder covered by Nb + 5% nanodiamond)	50:50 (45:5)	42-98	6

Table 3. The Vickers microhardness and the temperature of superconductive transition T_c of synthesized composite materials.

5.2 Nb_3Sn -diamond-system

An intermetallic Nb_3Sn compound crystallizes in cubic structure type A-15. Tin atoms are located in body-centered cubic positions, pairs of Nb atoms located on the cubic faces parallel to the coordinate axes (fig. 15). The unit cell contains 8 atoms: 2 Sn + 6Nb; the space group $Pm\bar{3}n$, $a_{cub.} = 0.529$ nm. Nb-atoms generate cross-cut chains (fig. 15a). The interatomic distance for Nb-atoms in one chain is appreciably less than the distance in the different chains. The chains of Nb-atoms respond for the generation of quasi one-dimensional electronic spectrum of d -state in this structure.

Nb_3Sn was mixed with micropowdered synthetic diamond and sintered at $P = 7.7$ GPa, $T = 1623$ K. The diffraction pattern in Fig. 16 shows that under high temperature and pressure Nb_3Sn partially decomposes to atoms of Nb and Sn. Metallic Nb creates NbC, while Sn in sample is in metallic state. It is worth to note that the temperature of synthesis 1623 K is much less than the melting temperature of Nb_3Sn (2400 K). It means that niobium carbide was synthesized in solid state without melting of metal. The content of metallic Sn is very

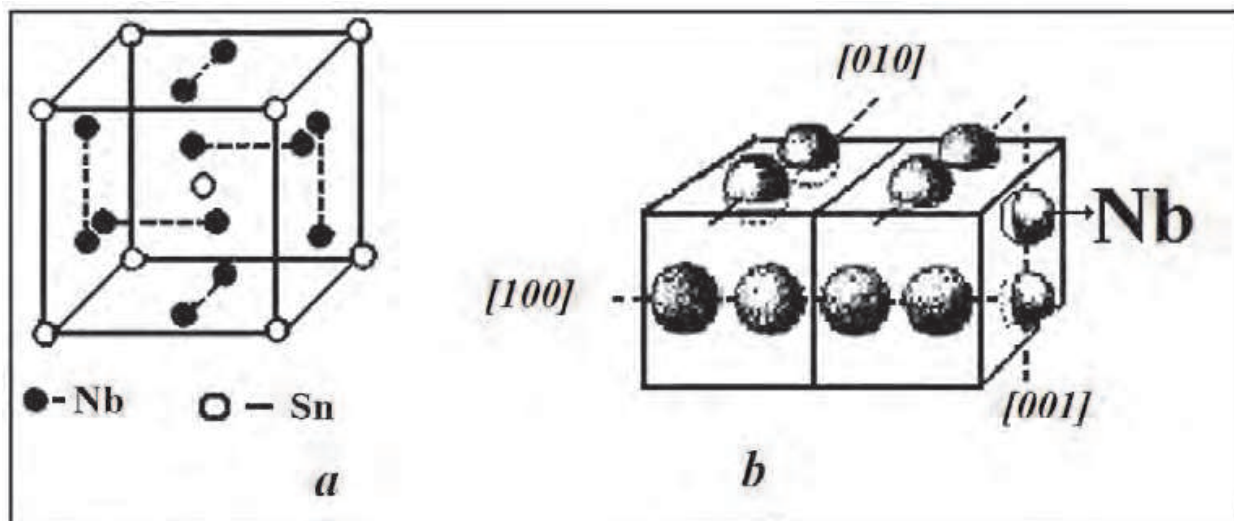


Fig. 15. The crystal structure of Nb₃Sn. *a* - Positions of atoms in the unit cell, *b* - chains of Nb-atoms. The coordinate axes are denoted in the *b*-part where two unit cell are painted.

small. Positions of diffractions peaks of Nb₃Sn correspond to the diffraction database (ICDD database PDF-2, card № 19-0875). Thus the decomposition of Nb₃Sn is insignificant in spite of high parameters of sintering. The composite Nb₃Sn with diamond powder is a superconductor with T_C about 15.5 K as it is shown in fig. 17. This value of T_C is close to the T_C of the initial Nb₃Sn.

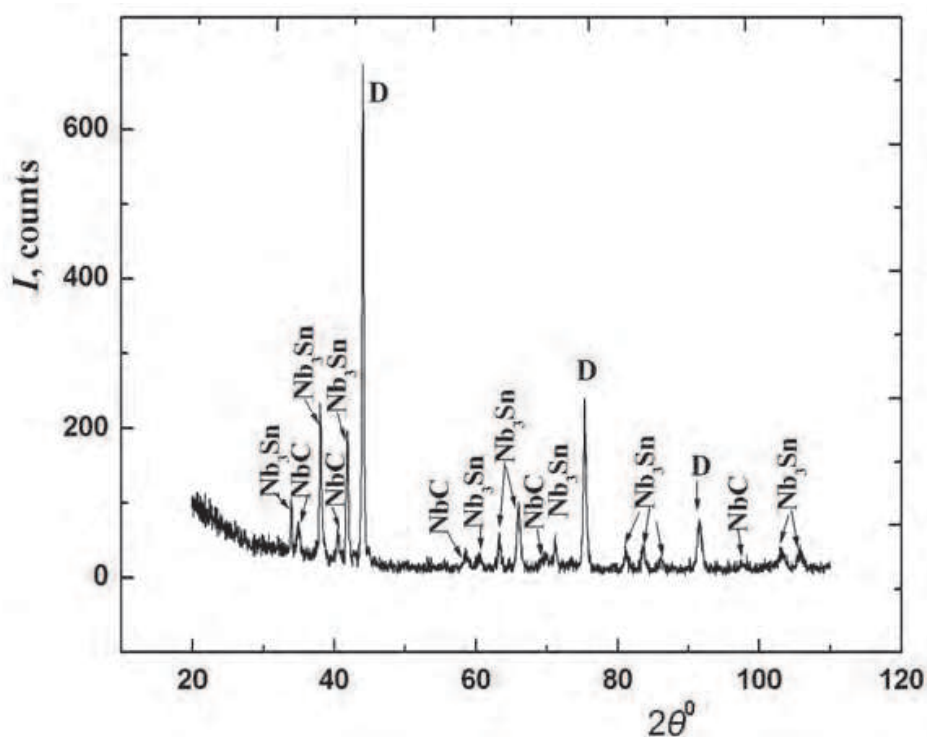


Fig. 16. X-ray diffraction pattern of (50%Nb₃Sn + 50% micropowder diamond) sample sintered at $P = 7.7$ GPa, $T = 1625$ K; D - reflections of diamond, NbC - reflections of niobium carbide.

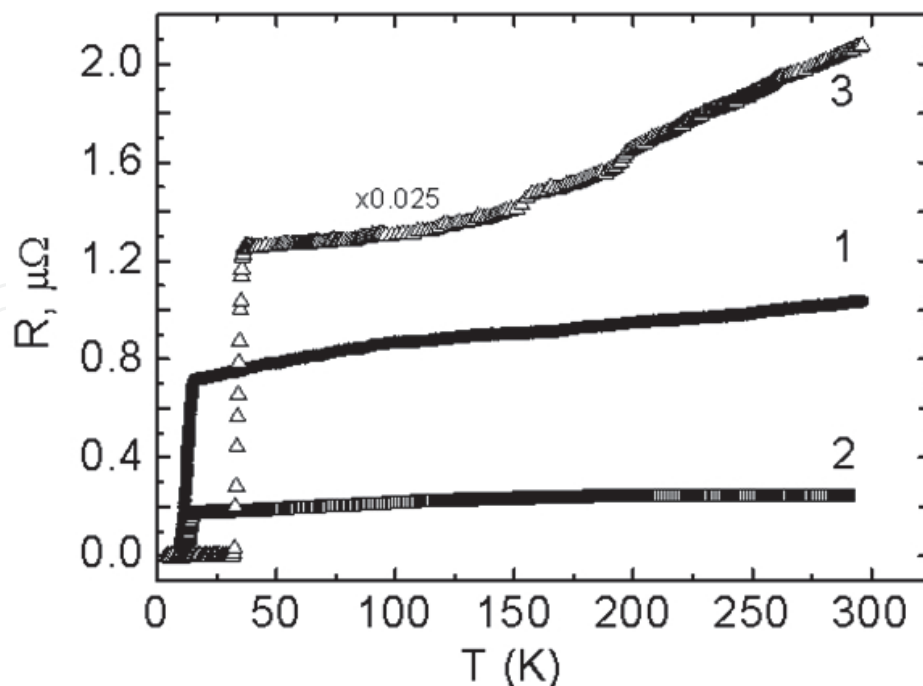


Fig. 17. Temperature dependence of resistance in different superhard composites: 1 - 50%Nb₃Sn + 50% micropowder diamond ($T_C=15.6$ K); 2 - 70%Nb₃Sn + 30% micropowder diamond ($T_C=15.5$ K) and 3 - MgB₂+cBN ($T_C=36.5$ K) for comparison.

6. Conclusion

The superhard superconducting composites are the new large family of materials for cryogenic electro-mechanical tools and devices. We employed high-pressure-high-temperature technique for synthesis of various superconducting composites on the basis of the hardest known materials: diamond, cubic boron nitride, C₆₀-fullerites. The best traditional superconductor alloys and relatively new, like MgB₂ have been used for synthesis to provide a superconductivity of the target materials. The structure and properties of the synthesized composites have been investigated. The highest values of microhardness up to 98 GPa and the highest elastic moduli have been found in diamond-based composites. Among them diamond-niobium composite is the hardest and it possesses 12.5K superconductor transition temperature. The highest $T_C = 37.5$ K has diamond-niobium-MgB₂ composite. The composites of superhard materials with conventional superconductor alloys like Ti₃₄Nb₆₆ and Nb₃Sn also possess superconductivity with the critical temperature 8.9 - 15.6 K. The optimal ratio of superconductor to superhard compounds in composites varies in the range from 20:80 to 50:50 wt%. The pressure and temperature parameters of synthesis are rather high: $P = 7.7 - 12.5$ GPa ; $T_s = 1373 - 2173$ K at the heating time $\tau = 60 - 90$ s. However it may be supposed that with the increase of τ the pressure and temperature of synthesis may be reduced substantially. The X-ray diffraction analysis revealed formation of metal carbides on the boundaries of diamond micro- and nanocrystals and nanocarbon phases originated from C₆₀ fullerene. The carbide phases provide strong chemical bonding of superconductor matrix with superhard carbon grains, thus the target composites possess very high strength. The obtained new composite materials can be successfully used in cryogenic

electro-mechanical systems and in cryogenic research devices. The unique high-strength superconducting anvils for research pressure-induced apparatus were made and employed for investigations of the pressure effect up to 22 GPa on the superconductor transition temperatures in the metallic high-pressure phase of GaP.

7. References

- Blank, V.; Buga, S.; Dubitsky, G.; Serebryanaya, N.; Popov, M. & Sundqvist, B. (1998). High-Pressure Polymerized Phases of C₆₀. *Carbon*, V. 36, No 4, (April 1998), pp. 319-343, ISSN 0008-6223
- Blank, V.; Buga, S.; Dubitsky, G.; Serebryanaya, N.; Prokhorov, V.; Mavrin, B.; Denisov, V.; Chernozatonskii, L.; Berezina, S. & Levin, V. (2006). Synthesis of Superhard and Ultrahard Materials by 3D-polymerization of C₆₀, C₇₀ Fullerenes under High Pressure (15 GPa) and Temperatures up to 1820 K. *Zeitschrift fur Naturforschung section B-A Journal of Chemical Sciences*, Vol. 61 b, No 12, (December 2006), pp. 1547-1554, ISSN 0932-0776
- Blank, V., Buga, S., Dubitsky, G., Gogolinsky, K., Prokhorov, V., Serebryanaya, N.; Popov, V. (2007). High-Pressure Synthesis of Carbon Nanostructured Superhard Materials., In: *Molecular Building Blocks for Nanotechnology*, Mansoori, A., George, T., Assoufid, L., Zhang, G., pp. 393-418. Springer Science+Business Media LLC, ISBN-10: 0-387-39937-2, New York, U.S.A.
- Buga, S.; Blank, V.; Dubitsky, G.; Edman, L.; Zhu, X.-M.; Nyeanchi, E. & Sundqvist, B. (2000). Semimetallic and Semiconductor Properties of Some Superhard and Ultrahard Fullerites in the Range 300–2 K. *Journal of Physics and Chemistry of Solids*, Vol. 61, No 7, (July 2000), pp. 1009-1015, ISSN 0022-3697
- Buga, S.; Blank, V.; Serebryanaya, N.; Dzwilewski, A.; Makarova, T. & Sundqvist, B. (2005). Electrical Properties of 3D-Polymeric Crystalline and Disordered C₆₀ and C₇₀ fullerites. *Diamond and Related Materials*, Vol. 14, Issue: 3-7, Special Issue: Sp. Iss. SI, (Mart-July 2005), pp. 896-901, ISSN 0925-9635
- Bulychev, B., Lunin, R., Krechetov, A., Kulbachinskii, V., Kytin, V., Pohlak, K., Lips, K.; Rappich, J. (2004) *J. Phys. Chem. Solids* Vol. 65, (2004) pp. 337-343
- Buzea, C. & Yamashita, T. (2001). Review of the Superconducting Properties of MgB₂. *Superconductor Science & Technology*, Vol. 14, No 11, (November 2001), pp. R115-R146, ISSN: 0953-2048
- Dou, S.; Yeoh, W.; Horvat, J. & Ionescu, M. (2003). Effect of Carbon Nanotube Doping on Critical Current Density of MgB₂ Superconductor. *Applied Physics Letters*, Vol. 83, No 24, (15 December 2003), pp.4996-4998, ISSN 0003-6951
- Dubitsky, G.; Blank, V.; Buga, S.; Semenova, E.; Kul'bachinskii, V.; Krechetov, A. & Kytin, V. (2005). Superhard Superconducting Materials Based on Diamond and Cubic Boron Nitride. *JETP Letters*, Vol. 81, No 6, (June 2005), pp. 323-326, ISSN 0021-3640
- Dubitsky, G.; Blank, V.; Buga, S.; Semenova, E., Serebryanaya, N.; Aksenkov, V.; Prokhorov, V.; Kul'bachinskii, V.; Krechetov, A. & Kytin, V. (2006). Superhard Superconductor Composites Obtained by Sintering of Diamond, c-BN and C₆₀ Powders with Superconductors. *Zeitschrift fur Naturforschung section B-A Journal of*

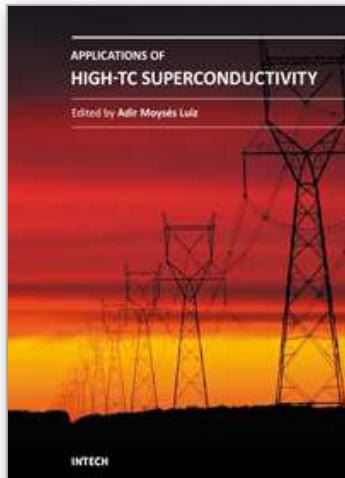
- Chemical Sciences*, Vol. 61 b, No 12, (December 2006), pp. 1541-1546, ISSN 0932-0776
- Dubrovinskaya, N., Eska, G., Sheshin, G., Braun, H.; (2006) Superconductivity in Polycrystalline Boron-doped Diamond Synthesized at 20 GPa and 2700K. *Journal of Applied Physics*, Vol. 99 (February 2006) pp. 0333903-1 -7, ISSN 0021-8979
- Ekimov, E.; Sidorov, V.; Bauer, E.; Mel'nik N.; Curro, N.; Thompson, J. & Stishov S. (2004). Superconductivity in Diamond. *Nature*, Vol. 428, No 6982, (April 2004), pp. 542-545, ISSN 0028-0836
- Gurevich, A.; Minc, R. & Rakhmanov, A. (1987). *Fizika kompositnyh sverhprovodnikov*, (Russian.), Nauka, Moscow, USSR
- Holczer, K. & Whetten, R. (1993). Superconducting and Normal State Properties of the A_3C_{60} Compounds, In: *The Fullerenes*, Kroto, H.; Fischer, J. & Cox, D., pp. 123-138. Pergamon Press, ISBN 0-08-042152-0, Oxford, UK
- Jung, C.; Park, M.-S.; Kang, W.; Kim, M.-S.; Kim, K.; Lee, S. & Lee, S.-I. (2001). Effect of Sintering Temperature under High Pressure on the Superconductivity of MgB_2 . *Applied Physics Letters*, Vol. 78, No 26, (25 June 2001), pp. 4157-4159, ISSN 0003-6951
- Karimov, Yu. & Utkina. (1990). Superconductivity of Nonstoichiometric Niobium Carbide. *Pis'ma v Zhurnal Eksperimental' i Teoreticheskoi Fiziki*, Vol. 51, No. 9, (May 1990), 468-470. (*Journal Experimental and Theoretical Physics Letters*, Vol. 51, No. 9, (May 1990), pp. 528-531, ISSN 0021-3640
- Krasnosvobodtsev, S.; Shabanova, N.; Ekimov, E.; Nozdrin, V. & Pechen', E. (1995). Critical Magnetic Field of NbC: New Data on Clean Superconductor Films. *Zhurnal Eksperimental' i Teoreticheskoi Fiziki*, Vol. 108, No. 3(9), (September 1995), pp.970-976. (*Journal Experimental and Theoretical Physics*, Vol. 81, No. 3, (September 1995), pp. 534-537, ISSN 1063-7761
- Kulbachinskii, V. (2004) . Electronic properties and superconductivity of low-dimensional carbon structures *Low Temperature Physics* Vol. 30 , No. 11, (November 2004), pp. 826-833.
- Kulbachinskii, V, Bulychev, B., Kytin, V., Krechetov, A., Konstantinova, E.; Lunin, R. (2008). Superconductivity, electron paramagnetic resonance, and Raman scattering studies of heterofullerides with Cs and Mg. *Advances in Condensed Matter Physics*— Vol. 2008 (2008), Article ID 941372, 6 pages doi:10.1155/2008/941372
- Kulbachinskii, V.; Buga, S.; Blank, V.; Dubitsky, G. & Serebryanaya N. (2010). Superconducting Superhard Composites Based on C_{60} , Diamond or Boron Nitride and MgB_2 . *Journal of Nanostructured Polymers and Nanocomposites*, Vol. 6, No. 4, (2010), pp. 119-122, ISSN 1790-4439
- Lyard, L.; Samuely, P.; Szabo, P.; Klein, T.; Marcenat, C.; Paulius, L.; Kim, K.; Jung, C.; Lee, H.; Kang, B.; Choi, S.; Lee, S.; Marcus, J.; Blanchard, S.; Jansen, A.; Welp, U.; Karapetrov, G. & Kwok, W. (2002). Anisotropy of the Upper Critical Field and Critical Current in Single Crystal MgB_2 . *Physical Review B*, Vol. 66, No. 18, (November 2002), pp. 180502(4), ISSN 0163-1829

- Nagamatsu, J.; Nakagawa, N.; Muranaka, T.; Zenitani, Y. & Akimitsu, J. (2001). *Nature*, Vol. 410, No. 6824, (March 2001), pp. 63-64, ISSN 0028-0836
- Narozhnyi, V.; Stepanov, G.; Dubitsky, G.; Semenova, E. & Yakovlev, E. (1988). Kamera Vysokogo Davleniya iz sverhprovodyaschego Materiala (in Russian). *Fizika I Tehnika Vysokih Davlenii*, No. 27, (1988), pp. 88-91, ISSN 0203-4654
- Pachla, W.; Kovac, P.; Diduszko, R.; Mazur, A.; Huek, I.; Morawski, A. & Presz, A. (2003). *Superconductor Science and Technology*, Vol. 16, No. 7, (January 2003), pp. 7-13, ISSN 0953-2048
- Pickett, W.; Klein, B. & Zeller, R. (1986). Electronic structure of the carbon vacancy in NbC. *Physical Review B*, Vol. 34, No. 4 (August 1986), pp. 2517-2521, ISSN 1098-0121
- Prikhna, T.; Gawalek, W.; Surzhenko, A.; Moshchil, V.; Sergienko, N.; Savchuk, Y.; Melnikov, V.; Nagorny, P.; Habisreuther, T.; Dub, S.; Wendt, M.; Litzkendorf, D.; Dellith, J.; Schmidt, C.; Krabbes, G. & Vlasenko, A. (2004) High-pressure Synthesis of MgB₂ with and without Tantalum Additions. *Physica C-Superconductivity and its Applications*, Vol. 372, (2004), pp. 1543-1545, ISSN: 0921-4534
- Prokhorov, V.; Blank, V.; Buga, S. & Levin, V. (1999) Scanning Acoustic Microscopy Study of Superhard C₆₀ Based Polymerized Fullerenes. *Synthetic Metals*, Vol. 103, No. 1-3, pp. 2439-2442, ISSN 0379-6779
- Shabanova, N.; Krasnosvobodtsev, S.; Nozdrin, V. & Golovashkin, A. (1996). Upper Critical Magnetic Field and Electron Characteristics of NbC, Nb₃Sn, RBa₂Cu₃O₇ Superconducting Compounds where (R=Y, Ho). *Fizika Tverdogo Tela*, Vol. 38, No. 7, (July 1996), pp. 1969-1985. (*Physics of the Solid State*, Vol.38, No. 7, pp.1085-, ISSN 1063-7834)
- Shul'zhenko, A.; Ginsburg, B.; Hovah, N. & Pruss, A. (1987). New Superhard Materials abroad (review) (in Russian). *Sverhtverdye Materialy*, No. 1, pp. 23-28, ISSN 0203-3119.
- Sidorov, V.; Ekimov, E.; Stishov, S.; Bauer, E. & Thompson, J. (2005). Superconducting and Normal-State Properties of Heavily Hole-Doped Diamond. *Physical Review B*, Vol. 71, No. 6, (June 2005), pp. 060502(4), Rapid Communications, ISSN 1098-0121
- Tampieri, A.; Celotti, G.; Sprio, S.; Caciuffo, R. & Rinaldi, D. (2004). Study of the Sintering Behavior of MgB₂ Superconductor During Hot-Pressing. *Physica C*, Vol. 400, No. 3, (2004), pp. 97-104, ISSN 0921-4534
- Toulemonde, P.; Musolino, N. & Flukiger, R. (2003). High-pressure Synthesis of Pure and Doped Superconducting MgB₂ compounds. *Superconductor Science & Technology*, Vol. 16, No. 2, (February 2003), pp. 231-236, ISSN 0953-2048
- Toth, L. (1971) *Transition Metal Carbides and Nitrides*. Academic, New York, 1971. (Mir, Moscow, 1974)
- Willens, R.; Boehler, E. & Matthias, B. (1967). Superconductivity of the Transition-Metal Carbides. *Physical Review*, Vol. 159, No. 2, (July 1967), pp. 327-330.
- Zenitani, Y. & Akimitsu, J. (2003). Discovery of the New Superconductor MgB₂ and its Recent Development. *Association Asia Pacific Physical Societies Bulletin*, Vol. 13, No. 1, (February 2003), pp. 26-33, ISSN 0218-2203.

Zhao, Y.; Cheng, C.; Rui, X.; Zhang, H.; Munroe, P.; Zeng, H.; Koshizuka, N. & Murakami, M. (2003). Improved Irreversibility Behavior and Critical Current Density in MgB₂-Diamond Nanocomposites. *Applied Physics Letters*, Vol. 83, No. 14, (October 2003), pp. 2916-2918, ISSN 0003-6951.

IntechOpen

IntechOpen



Applications of High-Tc Superconductivity

Edited by Dr. Adir Luiz

ISBN 978-953-307-308-8

Hard cover, 260 pages

Publisher InTech

Published online 27, June, 2011

Published in print edition June, 2011

This book is a collection of the chapters intended to study only practical applications of HTS materials. You will find here a great number of research on actual applications of HTS as well as possible future applications of HTS. Depending on the strength of the applied magnetic field, applications of HTS may be divided in two groups: large scale applications (large magnetic fields) and small scale applications (small magnetic fields). 12 chapters in the book are fascinating studies about large scale applications as well as small scale applications of HTS. Some chapters are presenting interesting research on the synthesis of special materials that may be useful in practical applications of HTS. There are also research about properties of high-Tc superconductors and experimental research about HTS materials with potential applications. The future of practical applications of HTS materials is very exciting. I hope that this book will be useful in the research of new radical solutions for practical applications of HTS materials and that it will encourage further experimental research of HTS materials with potential technological applications.

How to reference

In order to correctly reference this scholarly work, feel free to copy and paste the following:

Sergei Buga, Gennadii Dubitsky, Nadezhda Serebryanaya, Vladimir Kulbachinskii and Vladimir Blank (2011). Superhard Superconductive Composite Materials Obtained by High-Pressure-High-Temperature Sintering, Applications of High-Tc Superconductivity, Dr. Adir Luiz (Ed.), ISBN: 978-953-307-308-8, InTech, Available from: <http://www.intechopen.com/books/applications-of-high-tc-superconductivity/superhard-superconductive-composite-materials-obtained-by-high-pressure-high-temperature-sintering>

INTECH
open science | open minds

InTech Europe

University Campus STeP Ri
Slavka Krautzeka 83/A
51000 Rijeka, Croatia
Phone: +385 (51) 770 447
Fax: +385 (51) 686 166
www.intechopen.com

InTech China

Unit 405, Office Block, Hotel Equatorial Shanghai
No.65, Yan An Road (West), Shanghai, 200040, China
中国上海市延安西路65号上海国际贵都大饭店办公楼405单元
Phone: +86-21-62489820
Fax: +86-21-62489821

© 2011 The Author(s). Licensee IntechOpen. This chapter is distributed under the terms of the [Creative Commons Attribution-NonCommercial-ShareAlike-3.0 License](https://creativecommons.org/licenses/by-nc-sa/3.0/), which permits use, distribution and reproduction for non-commercial purposes, provided the original is properly cited and derivative works building on this content are distributed under the same license.

IntechOpen

IntechOpen